

Shot noise of charge and spin transport in a junction with a precessing molecular spin

Milena Filipović and Wolfgang Belzig

Fachbereich Physik, Universität Konstanz, D-78457 Konstanz, Germany

(Dated: April 6, 2018)

Magnetic molecules and nanomagnets can be used to influence the electronic transport in mesoscopic junction. In a magnetic field the precessional motion leads to resonances in the dc- and ac-transport properties of a nanocontact, in which the electrons are coupled to the precession. Quantities such as the dc conductance or the ac response provide valuable information, such as the level structure and the coupling parameters. Here, we address the current-noise properties of such contacts. This encompasses the charge current and spin-torque shot noise, which both show a steplike behavior as functions of bias voltage and magnetic field. The charge-current noise shows pronounced dips around the steps, which we trace back to interference effects of electrons in quasienergy levels coupled by the molecular spin precession. We show that some components of the noise of the spin-torque currents are directly related to the Gilbert damping and hence are experimentally accessible. Our results show that the noise characteristics allow us to investigate in more detail the coherence of spin transport in contacts containing magnetic molecules.

I. INTRODUCTION

Shot noise of charge current has become an active research topic in recent decades, since it enables the investigation of microscopic transport properties, which cannot be obtained from the charge current or conductance.¹ It has been demonstrated that spin-flip induced fluctuations in diffusive conductors connected to ferromagnetic leads enhance the noise power, approaching the Poissonian value.^{2,3} Accordingly, the Fano factor defined as $F = S(0)/e|I|$, which describes the deviation of the shot noise from the average charge current, equals 1 in this case. On the other hand, it has been shown that shot noise in a ferromagnet-quantum-dot-ferromagnet system with antiparallel magnetization alignments can be suppressed due to spin flip, with $F < 1/2$.⁴

The quantum-interference phenomenon, which is a manifestation of the wave nature of electrons, has attracted a lot of attention. The quantum-interference effects occur between coherent electron waves in nanoscale junctions.⁵ Quantum interference in molecular junctions influences their electronic properties.^{6–10} The Fano effect¹¹ due to the interference between a discrete state and the continuum has an important role in investigation of the interference effects in nanojunctions, which behave in an analogous way, and are manifested in the conductance or noise spectra.^{5,12,13} Particularly interesting examples involve spin-flip processes, such as in the presence of Rashba spin-orbit interaction,^{14,15} a rotating magnetic field,¹⁶ or in the case of the magnetotransport.^{17–19}

In the domain of spin transport it is interesting to investigate the noise properties, as the discrete nature of electron spin leads to the correlations between spin-carrying particles. The spin current is usually a nonconserved quantity that is difficult to measure, and its shot noise depends on spin-flip processes leading to spin-current correlations with opposite spins.^{20–22} The investigation of the spin-dependent scattering, spin accumulation,²³ and attractive or repulsive interactions in mesoscopic systems can be obtained using the shot

noise of spin current,²⁴ as well as measuring the spin relaxation time.^{20,24} Even in the absence of charge current, a nonzero spin current and its noise can still emerge.^{22,25,26} Several works have studied the shot noise of a spin current using, e.g., the nonequilibrium Green's functions method and scattering matrix theory.^{22,27–29}

It was demonstrated that the magnetization noise originates from transferred spin current noise via a fluctuating spin-transfer torque in ferromagnetic-normal-ferromagnetic systems,³⁰ and magnetic tunnel junctions.³¹ Experimentally, Spin Hall noise measurements have been demonstrated,³² and in a similar fashion the spin-current shot noise due to magnon currents can be related to the nonquantized spin of interacting magnons in ferri-, ferro-, and antiferromagnets.^{33,34} Quantum noise generated from the scatterings between the magnetization of a nanomagnet and spin-polarized electrons has been studied theoretically as well.^{35,36} The shot noise of spin-transfer torque was studied recently using a magnetic quantum dot connected to two non-collinear magnetic contacts.²⁹ According to the definition of the spin-transfer torque,^{37,38} both autocorrelations and cross-correlations of the spin-current components contribute to the spin-torque noise.

In this article, we study theoretically the noise of charge and spin currents and spin-transfer torque in a junction connected to two normal metallic leads. The transport occurs via a single electron energy level interacting with a molecular magnet in a constant magnetic field. The spin of the molecular magnet precesses around the magnetic field with the Larmor frequency, which is kept undamped, e.g., due to external driving. The electronic level may belong to a neighboring quantum dot or it may be an orbital of the molecular magnet itself. The electronic level and the molecular spin are coupled via exchange interaction. We derive expressions for the noise components using the Keldysh nonequilibrium Green's functions formalism.^{39–41} The noise of charge current is contributed by both elastic processes driven by the bias voltage, and inelastic tunneling processes driven by the

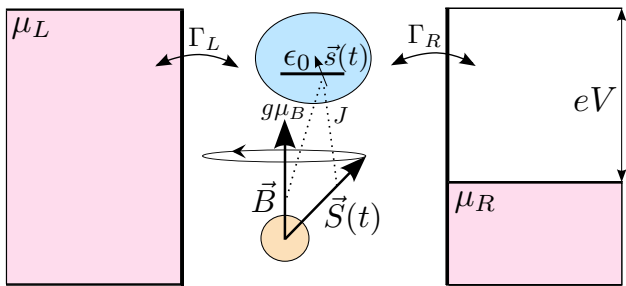


FIG. 1. (Color online) Tunneling through a single molecular level with energy ϵ_0 in the presence of a precessing molecular spin $\vec{S}(t)$ in a constant magnetic field \vec{B} , connected to two metallic leads with chemical potentials μ_ξ , $\xi = L, R$. The molecular level is coupled to the spin of the molecule via exchange interaction with the coupling constant J . The applied dc-bias voltage $eV = \mu_L - \mu_R$, and the tunnel rates are Γ_ξ .

molecular spin precession. We observe diplike features in the shot noise due to inelastic tunneling processes and destructive quantum interference between electron transport channels involved in the spin-flip processes. The driving mechanism of the correlations of the spin-torque components in the same spatial direction involves both precession of the molecular spin and the bias voltage. Hence, they are contributed by elastic and inelastic processes, with the change of energy equal to one or two Larmor frequencies. The nonzero correlations of the perpendicular spin-torque components are driven by the molecular spin precession, with contributions of spin-flip tunneling processes only. These components are related to the previously obtained Gilbert damping coefficient,^{42,43} which characterize the Gilbert damping term of the spin-transfer torque,^{44–46} at arbitrary temperature.

The article is organized as follows. The model and theoretical framework based on the Keldysh nonequilibrium Green's functions formalism^{39–41} are given in Sec. II. Here we derive expressions for the noise of spin and charge currents. In Sec. III we investigate and analyze the properties of the charge-current shot noise. In Sec. IV we derive and analyze the noise of spin-transfer torque. The conclusions are given in Sec. V.

II. MODEL AND THEORETICAL FRAMEWORK

The junction under consideration consists of a noninteracting single-level quantum dot in the presence of a precessing molecular spin in a magnetic field along the z -axis, $\vec{B} = B\vec{e}_z$, coupled to two noninteracting leads (Fig. 1). The junction is described by the Hamiltonian

$$\hat{H}(t) = \sum_{\xi \in \{L, R\}} \hat{H}_\xi + \hat{H}_T + \hat{H}_D(t) + \hat{H}_S, \quad (1)$$

where

$$\hat{H}_\xi = \sum_{k, \sigma} \epsilon_{k\xi} \hat{c}_{k\sigma\xi}^\dagger \hat{c}_{k\sigma\xi} \quad (2)$$

is the Hamiltonian of contact $\xi = L, R$. The spin-(up or down) state of the electrons is denoted by the subscript $\sigma = \uparrow, \downarrow = 1, 2 = \pm 1$. The tunnel coupling between the quantum dot and the leads reads

$$\hat{H}_T = \sum_{k, \sigma, \xi} [V_{k\xi} \hat{c}_{k\sigma\xi}^\dagger \hat{d}_\sigma + V_{k\xi}^* \hat{d}_\sigma^\dagger \hat{c}_{k\sigma\xi}], \quad (3)$$

with spin-independent matrix element $V_{k\xi}$. The creation (annihilation) operators of the electrons in the leads and the quantum dot are given by $\hat{c}_{k\sigma\xi}^\dagger$ ($\hat{c}_{k\sigma\xi}$) and \hat{d}_σ^\dagger (\hat{d}_σ). The Hamiltonian of the electronic level equals

$$\hat{H}_D(t) = \sum_{\sigma} \epsilon_0 \hat{d}_\sigma^\dagger \hat{d}_\sigma + g\mu_B \hat{s} \vec{B} + J \hat{s} \vec{S}(t). \quad (4)$$

The first term in Eq. (4) is the Hamiltonian of the noninteracting single-level quantum dot with energy ϵ_0 . The second term describes the electronic spin in the dot, $\hat{s} = (\hbar/2) \sum_{\sigma\sigma'} (\vec{\sigma})_{\sigma\sigma'} \hat{d}_\sigma^\dagger \hat{d}_{\sigma'}$, in the presence of a constant magnetic field \vec{B} , and the third term represents the exchange interaction between the electronic spin and the molecular spin $\vec{S}(t)$. The vector of the Pauli matrices is given by $\hat{\sigma} = (\hat{\sigma}_x, \hat{\sigma}_y, \hat{\sigma}_z)^T$. The g -factor of the electron and the Bohr magneton are g and μ_B , whereas J is the exchange coupling constant between the electronic and molecular spins.

The last term of Eq. (1) can be written as

$$\hat{H}_S = g\mu_B \vec{S} \vec{B}, \quad (5)$$

and represents the energy of the molecular spin \vec{S} in the magnetic field \vec{B} . We assume that $|\vec{S}| \gg \hbar$ and neglecting quantum fluctuations treat \vec{S} as a classical variable. The magnetic field \vec{B} generates a torque on the spin \vec{S} that causes the spin to precess around the field axis with Larmor frequency $\omega_L = g\mu_B B/\hbar$. The dynamics of the molecular spin is kept constant, which can be realized, e.g., by external rf fields⁴⁷ to cancel the loss of magnetic energy due to the interaction with the itinerant electrons. Thus, the precessing spin $\vec{S}(t)$ pumps spin currents into the leads, but its dynamics remains unaffected by the spin currents, i.e., the spin-transfer torque exerted on the molecular spin is compensated by the above mentioned external means. The undamped precessional motion of the molecular spin, supported by the external sources, is then given by $\vec{S}(t) = S_\perp \cos(\omega_L t) \vec{e}_x + S_\perp \sin(\omega_L t) \vec{e}_y + S_z \vec{e}_z$, with θ the tilt angle between \vec{B} and \vec{S} , and $S_\perp = S \sin(\theta)$ the magnitude of the instantaneous projection of $\vec{S}(t)$ onto the xy plane. The component of the molecular spin along the field axis equals $S_z = S \cos(\theta)$.

The charge- and spin-current operators of the lead ξ are given by the Heisenberg equation^{39,40}

$$\hat{I}_{\xi\nu}(t) = q_\nu \frac{d\hat{N}_{\xi\nu}}{dt} = q_\nu \frac{i}{\hbar} [\hat{H}, \hat{N}_{\xi\nu}], \quad (6)$$

where $[\ , \]$ denotes the commutator, while $\hat{N}_{L\nu} = \sum_{k,\sigma,\sigma'} \hat{c}_{k\sigma L}^\dagger (\sigma_\nu)_{\sigma\sigma'} \hat{c}_{k\sigma' L}$ is the charge ($\nu = 0$ and $q_0 = -e$) and spin ($\nu = x, y, z$ and $q_{\nu \neq 0} = \hbar/2$) occupation number operator of the contact ξ . Here $\hat{\sigma}_0 = \hat{1}$ is the identity matrix. Taking into account that only the tunneling Hamiltonian \hat{H}_T generates a nonzero commutator in Eq. (6), the current operator $\hat{I}_{\xi\nu}(t)$ can be expressed as

$$\hat{I}_{\xi\nu}(t) = -q_\nu \frac{i}{\hbar} \sum_{\sigma,\sigma'} (\sigma_\nu)_{\sigma\sigma'} \hat{I}_{\xi,\sigma\sigma'}(t), \quad (7)$$

where the operator component $\hat{I}_{\xi,\sigma\sigma'}(t)$ equals

$$\hat{I}_{\xi,\sigma\sigma'}(t) = \sum_k [V_{k\xi} \hat{c}_{k\sigma\xi}^\dagger(t) \hat{d}_{\sigma'}(t) - V_{k\xi}^* \hat{d}_{\sigma'}^\dagger(t) \hat{c}_{k\sigma'\xi}(t)]. \quad (8)$$

The nonsymmetrized noise of charge and spin current is defined as the correlation between fluctuations of currents $I_{\xi\nu}$ and $I_{\zeta\mu}$,^{1,40}

$$S_{\xi\zeta}^{\nu\mu}(t, t') = \langle \delta \hat{I}_{\xi\nu}(t) \delta \hat{I}_{\zeta\mu}(t') \rangle, \quad (9)$$

with $\nu = \mu = 0$ for the charge-current noise. The fluctuation operator of the charge and spin current in lead ξ is given by

$$\delta \hat{I}_{\xi\nu}(t) = \hat{I}_{\xi\nu}(t) - \langle \hat{I}_{\xi\nu}(t) \rangle. \quad (10)$$

Using Eqs. (7) and (10), the noise becomes

$$S_{\xi\zeta}^{\nu\mu}(t, t') = -\frac{q_\nu q_\mu}{\hbar^2} \sum_{\sigma\sigma'} \sum_{\lambda\eta} (\sigma_\nu)_{\sigma\sigma'} (\sigma_\mu)_{\lambda\eta} S_{\xi\zeta}^{\sigma\sigma',\lambda\eta}(t, t'), \quad (11)$$

where $S_{\xi\zeta}^{\sigma\sigma',\lambda\eta}(t, t') = \langle \delta \hat{I}_{\xi,\sigma\sigma'}(t) \delta \hat{I}_{\zeta,\lambda\eta}(t') \rangle$. The formal expression for $S_{\xi\zeta}^{\nu\mu}(t, t')$ is given by Eq. (A10) in the Appendix, where it is obtained using Eq. (11) and Eqs. (A1)–(A9).

Using Fourier transformations of the central-region Green's functions given by Eqs. (A6)–(A8) and self-energies in the wide-band limit, the correlations given by Eq. (A9) can be further simplified. Some correlation functions are not just functions of time difference $t - t'$. Thus, as in Ref. 48, we used Wigner representation assuming that in experiments fluctuations are measured on timescales much larger than the driving period $\mathcal{T} = 2\pi/\omega_L$, which is the period of one molecular spin precession. The Wigner coordinates are given by $T' = (t + t')/2$ and $\tau = t - t'$, while the correlation functions are defined as

$$S_{\xi\zeta}^{\sigma\sigma',\lambda\eta}(\tau) = \frac{1}{\mathcal{T}} \int_0^{\mathcal{T}} dt \langle \delta \hat{I}_{\xi,\sigma\sigma'}(t + \tau) \delta \hat{I}_{\zeta,\lambda\eta}(t) \rangle. \quad (12)$$

The Fourier transform of $S_{\xi\zeta}^{\sigma\sigma',\lambda\eta}(\tau)$ is given by

$$S_{\xi\zeta}^{\sigma\sigma',\lambda\eta}(\Omega, \Omega') = 2\pi \delta(\Omega - \Omega') S_{\xi\zeta}^{\sigma\sigma',\lambda\eta}(\Omega), \quad (13)$$

where

$$S_{\xi\zeta}^{\sigma\sigma',\lambda\eta}(\Omega) = \int d\tau e^{i\Omega\tau} S_{\xi\zeta}^{\sigma\sigma',\lambda\eta}(\tau). \quad (14)$$

For the correlations which depend only on $t - t'$, the Wigner representation is identical to the standard representation.

The symmetrized noise of charge and spin currents reads^{1,40}

$$S_{\xi\zeta S}^{\nu\mu}(t, t') = \frac{1}{2} \langle \{ \delta \hat{I}_{\xi\nu}(t), \delta \hat{I}_{\zeta\mu}(t') \} \rangle, \quad (15)$$

where $\{, \}$ denotes the anticommutator. According to Eqs. (11), (12), (14), and (15), in the Wigner representation the nonsymmetrized noise spectrum reads

$$\begin{aligned} S_{\xi\zeta}^{\nu\mu}(\Omega) &= \int d\tau e^{i\Omega\tau} S_{\xi\zeta}^{\nu\mu}(\tau) \\ &= \int d\tau e^{i\Omega\tau} \frac{1}{\mathcal{T}} \int_0^{\mathcal{T}} dt \langle \delta \hat{I}_{\xi\nu}(t + \tau) \delta \hat{I}_{\zeta\mu}(t) \rangle \\ &= -\frac{q_\nu q_\mu}{\hbar^2} \sum_{\sigma\sigma'} \sum_{\lambda\eta} (\sigma_\nu)_{\sigma\sigma'} (\sigma_\mu)_{\lambda\eta} S_{\xi\zeta}^{\sigma\sigma',\lambda\eta}(\Omega), \end{aligned} \quad (16)$$

while the symmetrized noise spectrum equals

$$\begin{aligned} S_{\xi\zeta S}^{\nu\mu}(\Omega) &= \frac{1}{2} [S_{\xi\zeta}^{\nu\mu}(\Omega) + S_{\xi\zeta}^{\mu\nu}(-\Omega)] \\ &= -\frac{q_\nu q_\mu}{2\hbar^2} \sum_{\sigma\sigma'} \sum_{\lambda\eta} (\sigma_\nu)_{\sigma\sigma'} (\sigma_\mu)_{\lambda\eta} S_{\xi\zeta S}^{\sigma\sigma',\lambda\eta}(\Omega), \end{aligned} \quad (17)$$

where $S_{\xi\zeta S}^{\sigma\sigma',\lambda\eta}(\Omega) = [S_{\xi\zeta}^{\sigma\sigma',\lambda\eta}(\Omega) + S_{\xi\zeta}^{\lambda\eta,\sigma\sigma'}(-\Omega)]/2$. The experimentally most easily accessible quantity is the zero-frequency noise power.

III. SHOT NOISE OF CHARGE CURRENT

For the charge-current noise, it is convenient to drop the superscripts $\nu = \mu = 0$. The charge-current noise spectrum can be obtained as²⁴

$$S_{\xi\zeta}(\Omega) = -\frac{e^2}{\hbar^2} [S_{\xi\zeta}^{11,11} + S_{\xi\zeta}^{11,22} + S_{\xi\zeta}^{22,11} + S_{\xi\zeta}^{22,22}](\Omega). \quad (18)$$

In this section, we analyze the zero-frequency noise power of the charge current $S_{\xi\zeta} = S_{\xi\zeta}(0)$ at zero temperature. Taking into account that thermal noise disappears at zero temperature, the only contribution to the charge-current noise comes from the shot noise. The tunnel couplings between the molecular orbital and the leads, $\Gamma_\xi(\epsilon) = 2\pi \sum_k |V_{k\xi}|^2 \delta(\epsilon - \epsilon_{k\xi})$, are considered symmetric and in the wide-band limit $\Gamma_L = \Gamma_R = \Gamma/2$.

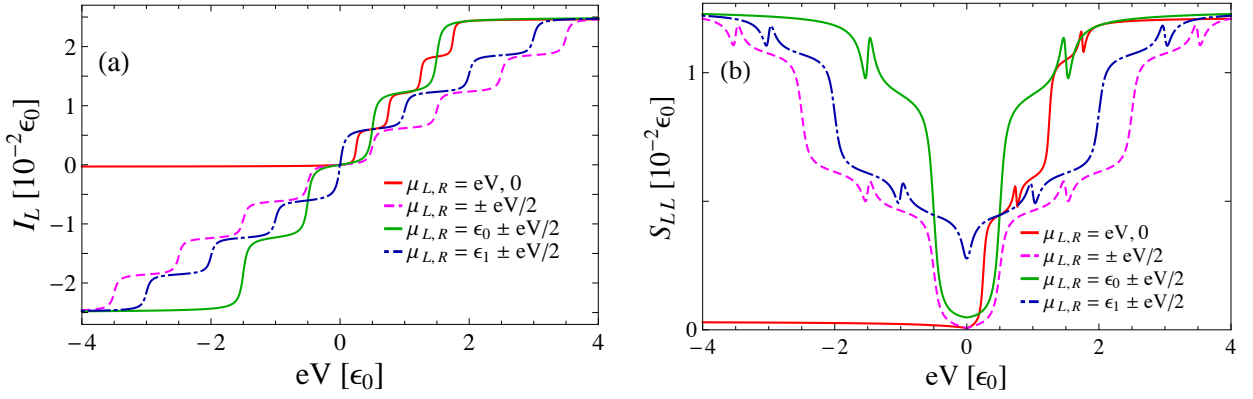


FIG. 2. (Color online) (a) Charge current I_L and (b) auto-correlation shot noise S_{LL} as functions of bias-voltage eV . All plots are obtained at zero temperature, with $\vec{B} = B\vec{e}_z$. The other parameters are $\Gamma_L = \Gamma_R = \Gamma/2$, $\Gamma = 0.05 \epsilon_0$, $\omega_L = 0.5 \epsilon_0$, $J = 0.01 \epsilon_0$, $S = 100$, and $\theta = \pi/2$. The molecular quasienergy levels are located at $\epsilon_1 = 0.25 \epsilon_0$, $\epsilon_2 = 0.75 \epsilon_0$, $\epsilon_3 = 1.25 \epsilon_0$, and $\epsilon_4 = 1.75 \epsilon_0$.

The average charge current from lead ξ can be expressed as

$$I_\xi = \frac{e\Gamma_\xi\Gamma_\zeta}{\hbar} \int \frac{d\epsilon}{2\pi} [f_\xi(\epsilon) - f_\zeta(\epsilon)] \times \sum_{\substack{\sigma\sigma' \\ \sigma \neq \sigma'}} \frac{|G_{\sigma\sigma}^{0r}(\epsilon)|^2 [1 + \gamma^2 |G_{\sigma'\sigma'}^{0r}(\epsilon + \sigma'\omega_L)|^2]}{|1 - \gamma^2 G_{\sigma\sigma}^{0r}(\epsilon) G_{\sigma'\sigma'}^{0r}(\epsilon + \sigma'\omega_L)|^2}, \quad (19)$$

where $\xi \neq \zeta$, while $G_{\sigma\sigma}^{0r}(\epsilon)$ are matrix elements of $\hat{G}^{0r}(\epsilon) = [\epsilon - \epsilon_0 + i \sum_\xi \Gamma_\xi/2 - \hat{\sigma}_z(g\mu_B B + JS_z)/2]^{-1}$.^{49,50} In the above expression, $f_\xi(\epsilon) = [e^{(\epsilon - \mu_\xi)/k_B T} + 1]^{-1}$ is the Fermi-Dirac distribution of the electrons in lead ξ , with k_B the Boltzmann constant and T the temperature. The conservation of the charge current implies that $S_{LL}(0) + S_{LR}(0) = 0$. Thus, it is sufficient to study only one correlation function.

Tuning the parameters in the system such as the bias voltage $eV = \mu_L - \mu_R$ (where μ_L and μ_R are the chemical potentials of the leads), \vec{B} , and the tilt angle θ , the shot noise can be controlled and minimized. The shot noise in the small precession frequency limit $\omega_L \ll k_B T$ is in agreement with Ref. 22 for $eV = 0$.

In Fig. 2(a) we present the average charge current as a staircase function of bias voltage, where the bias is varied in four different ways. In the presence of the external magnetic field and the precessing molecular spin, the initially degenerate electronic level with energy ϵ_0 results in four nondegenerate transport channels, which has an important influence on the noise. Each step corresponds to a new available transport channel. The transport channels are located at the Floquet quasienergies⁴³ $\epsilon_1 = \epsilon_0 - (\omega_L/2) - (JS/2)$, $\epsilon_2 = \epsilon_0 + (\omega_L/2) - (JS/2)$, $\epsilon_3 = \epsilon_0 - (\omega_L/2) + (JS/2)$, and $\epsilon_4 = \epsilon_0 + (\omega_L/2) + (JS/2)$, which are calculated using the Floquet theorem.^{16,51-54}

The correlated current fluctuations give nonzero noise power, which is presented in Fig. 2(b). The noise power shows the molecular quasienergy spectrum, and each step

or diplike feature in the noise denotes the energy of a new available transport channel. The noise has two steps and two diplike features that correspond to these resonances. Charge current and noise power are saturated for large bias voltages. If the Fermi levels of the leads lie below the resonances, the shot noise approaches zero for $eV \rightarrow 0$ [red and dashed pink lines in Fig. 2(b)]. This is due to the fact that a small number of electron states can participate in transport inside this small bias window and both current and noise are close to 0. If the bias voltage is varied with respect to the resonant energy ϵ_1 such that $\mu_{L,R} = \epsilon_1 \pm eV/2$ [dot-dashed blue line in Fig. 2(b)], or with respect to ϵ_0 such that $\mu_{L,R} = \epsilon_0 \pm eV/2$ [green line in Fig. 2(b)], we observe a valley at zero bias $eV = 0$, which corresponds to $\mu_L = \mu_R = \epsilon_1$ in the first case, and nonzero noise in the second case. For $eV = 0$, the charge current is zero, but the precession-assisted inelastic processes involving the absorption of an energy quantum ω_L give rise to the noise here.

At small bias voltage, the Fano factor $F = S_{LL}/e|I_L|$ is inversely proportional to eV and hence diverges as $eV \rightarrow 0$, indicating that the noise is super-Poissonian, as depicted in Fig. 3. Due to absorption (emission) processes¹⁶ and quantum interference effects, the Fano factor is a deformed steplike function, where each step corresponds to a resonance. As the bias voltage is increased, the noise is enhanced since the number of the correlated electron pairs increases with the increase of the Fermi level. For larger bias, due to the absorption and emission of an energy quantum ω_L , electrons can jump to a level with higher energy or lower level during the transport, and the Fano factor $F < 1$ indicates the sub-Poissonian noise. Around the resonances $\mu_{L,R} = \epsilon_i$, $i = 1, 2, 3, 4$, the probability of transmission is very high, resulting in the small Fano factor. Elastic tunneling contributes to the sub-Poissonian Fano factor around the resonances and competes with the spin-flip events caused by the molecular spin precession. However, if the reso-

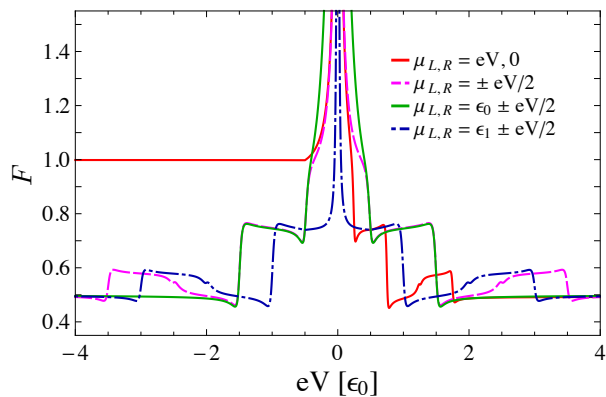


FIG. 3. (Color online) Fano factor F as a function of bias-voltage eV . All plots are obtained at zero temperature, with $\vec{B} = B\vec{e}_z$. The other parameters are set to $\Gamma = 0.05 \epsilon_0$, $\Gamma_L = \Gamma_R = \Gamma/2$, $\omega_L = 0.5 \epsilon_0$, $J = 0.01 \epsilon_0$, $S = 100$, and $\theta = \pi/2$. The positions of the molecular quasienergy levels are $\epsilon_1 = 0.25 \epsilon_0$, $\epsilon_2 = 0.75 \epsilon_0$, $\epsilon_3 = 1.25 \epsilon_0$, and $\epsilon_4 = 1.75 \epsilon_0$.

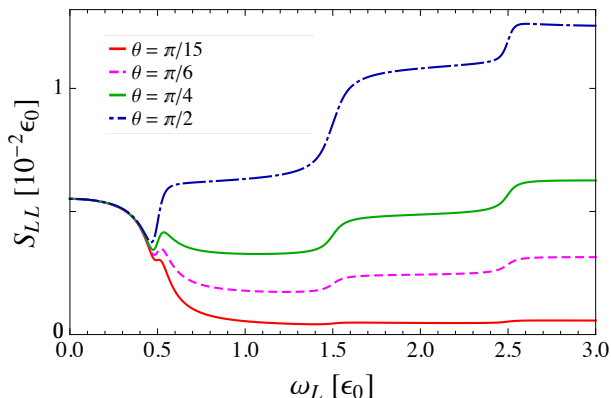


FIG. 4. (Color online) Shot noise of charge current S_{LL} as a function of the Larmor frequency ω_L for different tilt angles θ , with $\vec{B} = B\vec{e}_z$, at zero temperature. The other parameters are $\Gamma = 0.05 \epsilon_0$, $\Gamma_L = \Gamma_R = \Gamma/2$, $\mu_L = 0.75 \epsilon_0$, $\mu_R = 0.25 \epsilon_0$, $J = 0.01 \epsilon_0$, and $S = 100$. For $\omega_L = \mu_L - \mu_R$, we observe a dip due to destructive quantum interference.

nant quasienergy levels are much higher than the Fermi energy of the leads, the probability of transmission is very low and the Fano factor is close to 1, as shown in Fig. 3 (red line). This means that the stochastic processes are uncorrelated. If the two levels connected with the inelastic photon emission (absorption) tunnel processes, or all four levels, lie between the Fermi levels of the leads, the Fano factor approaches $1/2$, which is in agreement with Ref. 55. For $eV = \epsilon_3$ [see Fig. 3 (red line)] a spin-down electron can tunnel elastically, or inelastically in a spin-flip process, leading to the increase of the Fano factor. Spin-flip processes increase the electron traveling time, leading to sub-Poissonian noise. Similarly, the Pauli exclusion principle is known to lead to sub-Poissonian noise, since it prevents the double occupancy of a level.

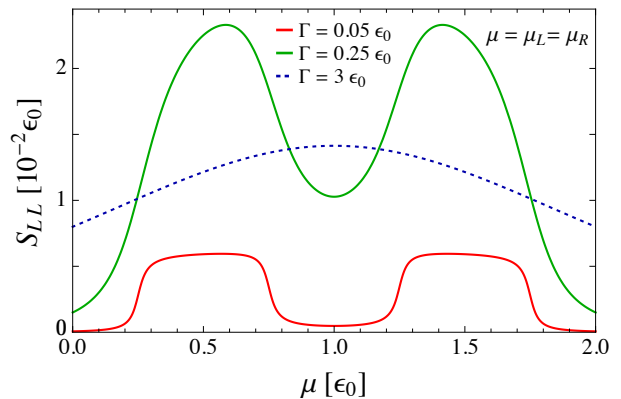


FIG. 5. (Color online) Shot noise of charge current S_{LL} as a function of the chemical potential of the leads $\mu = \mu_L = \mu_R$, with $\vec{B} = B\vec{e}_z$, for three different couplings Γ , where $\Gamma_L = \Gamma_R = \Gamma/2$, at zero temperature. The other parameters are $\omega_L = 0.5 \epsilon_0$, $J = 0.01 \epsilon_0$, $S = 100$, and $\theta = \pi/2$. The molecular quasienergy levels are positioned at $\epsilon_1 = 0.25 \epsilon_0$, $\epsilon_2 = 0.75 \epsilon_0$, $\epsilon_3 = 1.25 \epsilon_0$, and $\epsilon_4 = 1.75 \epsilon_0$.

The precessing molecular spin induces quantum interference between the transport channels connected with spin-flip events and the change of energy by one energy quantum ω_L , i.e., between levels with energies ϵ_1 and $\epsilon_2 = \epsilon_1 + \omega_L$, or ϵ_3 and $\epsilon_4 = \epsilon_3 + \omega_L$. The destructive quantum-interference effects manifest themselves in the form of diplike features in Fig. 2(b). When one or both pairs of the levels connected with spin-flip events enter the bias-voltage window, then an electron from the left lead can tunnel through both levels via elastic or inelastic spin-flip processes. Different tunneling pathways ending in the final state with the same energy destructively interfere, similarly as in the Fano effect.¹¹ Namely, the state with lower energy ϵ_1 (or ϵ_3) mimics the discrete state in the Fano effect. An electron tunnels into the state ϵ_1 (or ϵ_3), undergoes a spin flip and absorbs an energy quantum ω_L . The other state with energy ϵ_2 (or ϵ_4) is an analog of the continuum in the Fano effect, and the electron tunnels elastically through this level. These two tunneling processes (one elastic and the other inelastic) interfere, leading to a diplike feature in the noise power. If we vary, for instance, the bias-voltage as $eV = \mu_L$, where $\mu_R = 0$ [Fig. 2(b), red line], we observe diplike features for $eV = \epsilon_2$ and $eV = \epsilon_4$.

The destructive interference effect is also presented in Fig. 4, where noise power S_{LL} is depicted as a function of ω_L . Here, we observe a dip due to the quantum-interference effect around $\omega_L = 0.5 \epsilon_0$, which corresponds to $\mu_L = \epsilon_2$ and $\mu_R = \epsilon_1$. The other two steps in Fig. 4 occur when the Fermi energy of the right or left lead is in resonance with one of the quasienergy levels. The magnitude of the precessing component of the molecular spin, which induces spin-flip processes between molecular quasienergy levels, equals $JS \sin(\theta)/2$. Therefore, the dip increases with the increase of the tilt angle θ , and it

is maximal and distinct for $\theta = \pi/2$.

Finally, in Fig. 5 we plotted the noise power of charge current S_{LL} as a function of $\mu = \mu_L = \mu_R$ at zero temperature. It shows a nonmonotonic dependence on the tunneling rates Γ . For small Γ (Fig. 5, red line) the noise is increased if μ is positioned between levels connected with spin-flip events, and is contributed only by absorption processes of an energy quantum ω_L as we vary the chemical potentials. For larger Γ (Fig. 5, green line), the charge-current noise is increased since levels broaden and overlap, and more electrons can tunnel. With further increase of Γ (Fig. 5, dotted blue line) the noise starts to decrease, and it is finally suppressed for $\Gamma \gg \omega_L$ since a current-carrying electron sees the molecular spin as nearly static in this case, leading to a reduction of the inelastic spin-flip processes.

IV. SHOT NOISE OF SPIN CURRENT AND SPIN-TRANSFER TORQUE

In this section we present the spin-current noise spectrum components and relations between them. Later we introduce the noise of spin-transfer torque and we investigate the zero-frequency spin-torque shot noise at zero temperature. The components of the nonsymmetrized spin-current noise spectrum read

$$S_{\xi\zeta}^{xx}(\Omega) = -\frac{1}{4}[S_{\xi\zeta}^{12,21} + S_{\xi\zeta}^{21,12}](\Omega), \quad (20)$$

$$S_{\xi\zeta}^{xy}(\Omega) = -\frac{i}{4}[S_{\xi\zeta}^{12,21} - S_{\xi\zeta}^{21,12}](\Omega), \quad (21)$$

$$S_{\xi\zeta}^{zz}(\Omega) = -\frac{1}{4}[S_{\xi\zeta}^{11,11} - S_{\xi\zeta}^{11,22} - S_{\xi\zeta}^{22,11} + S_{\xi\zeta}^{22,22}](\Omega), \quad (22)$$

where Eq. (22) denotes the noise of the z component of the spin current.^{22,24} Since the polarization of the spin current precesses in the xy plane, the remaining components of the spin-current noise spectrum satisfy the following relations:

$$S_{\xi\zeta}^{yy}(\Omega) = S_{\xi\zeta}^{xx}(\Omega), \quad (23)$$

$$S_{\xi\zeta}^{yx}(\Omega) = -S_{\xi\zeta}^{xy}(\Omega), \quad (24)$$

$$S_{\xi\zeta}^{xz}(\Omega) = S_{\xi\zeta}^{zx}(\Omega) = S_{\xi\zeta}^{yz}(\Omega) = S_{\xi\zeta}^{zy}(\Omega) = 0. \quad (25)$$

Taking into account that the spin current is not a conserved quantity, it is important to notice that the complete information from the noise spectrum can be obtained by studying both the autocorrelation noise spectrum $S_{\xi\xi}^{jk}(\Omega)$ and cross-correlation noise spectrum $S_{\xi\zeta}^{jk}(\Omega)$, $\zeta \neq \xi$. Therefore, it is more convenient to investigate the spin-torque noise spectrum, where both autocorrelation and cross-correlation noise components of spin currents are included. The spin-transfer torque operator can be defined as

$$\hat{T}_j = -(\hat{I}_{Lj} + \hat{I}_{Rj}), \quad j = x, y, z; \quad (26)$$

while its fluctuation reads

$$\delta\hat{T}_j(t) = -[\delta\hat{I}_{Lj}(t) + \delta\hat{I}_{Rj}(t)]. \quad (27)$$

Accordingly, the nonsymmetrized and symmetrized spin-torque noise can be obtained using the spin-current noise components as

$$S_T^{jk}(t, t') = \langle \delta\hat{T}_j(t) \delta\hat{T}_k(t') \rangle \\ = \sum_{\xi\zeta} S_{\xi\zeta}^{jk}(t, t'), \quad j, k = x, y, z; \quad (28)$$

$$S_{TS}^{jk}(t, t') = \frac{1}{2}[S_T^{jk}(t, t') + S_T^{kj}(t', t)], \quad (29)$$

with the corresponding noise spectrums given by

$$S_T^{jk}(\Omega) = \sum_{\xi\zeta} S_{\xi\zeta}^{jk}(\Omega), \quad (30)$$

$$S_{TS}^{jk}(\Omega) = \sum_{\xi\zeta} S_{\xi\zeta S}^{jk}(\Omega). \quad (31)$$

According to Eqs. (23), (24), and (30), $S_T^{xx}(\Omega) = S_T^{yy}(\Omega)$ and $S_T^{xy}(\Omega) = -S_T^{yx}(\Omega)$.

In the remainder of the section we investigate the zero-frequency spin-torque shot noise $S_T^{jk} = S_T^{jk}(0)$ at zero temperature, where $S_T^{xx}(0) = S_{TS}^{xx}(0)$, $S_T^{yy}(0) = S_{TS}^{yy}(0)$, $S_T^{zz}(0) = S_{TS}^{zz}(0)$, while $S_T^{xy}(0)$ is a complex imaginary function, and $S_{TS}^{xy}(0) = 0$ according to Eqs. (24) and (31). Since $S_T^{xx}(0) = S_T^{yy}(0)$, all results and discussions related to $S_T^{xx}(0)$ also refer to $S_T^{yy}(0)$.

Spin currents $I_{\xi x}$ and $I_{\xi y}$ are periodic functions of time, with period $\mathcal{T} = 2\pi/\omega_L$, while $I_{\xi z}$ is time-independent. It has already been demonstrated that spin-flip processes contribute to the noise of spin current.²² The presence of the precessing molecular spin affects the spin-current noise. Since the number of particles with different spins changes due to spin-flip processes, additional spin-current fluctuations are generated. Currents with the same and with different spin orientations are correlated during transport. Due to the precessional motion of the molecular spin, inelastic spin currents with spin-flip events induce noise of spin currents and spin-torque noise, which can be nonzero even for $eV = 0$. The noise component S_T^{xy} is induced by the molecular spin precession and vanishes for a static molecular spin. The noises of spin currents and spin-transfer torque are driven by the bias voltage and by the molecular spin precession. Hence, in the case when both the molecular spin is static (absence of inelastic spin-flip processes) and $eV = 0$ (no contribution of elastic tunneling processes), they are all equal to zero. The noise of spin-transfer torque can be modified by adjusting system parameters such as the bias voltage eV , the magnetic field \vec{B} , or the tilt angle θ .

In Fig. 6 we present the zero-frequency spin-torque noise components $S_T^{xx} = S_T^{yy}$, $\text{Im}\{S_T^{xy}\}$, and S_T^{zz} as functions of the bias voltage $eV = \mu_L - \mu_R$, for $\mu_R = 0$ and different tilt angles θ between \vec{B} and \vec{S} at zero temperature. They give information on available transport

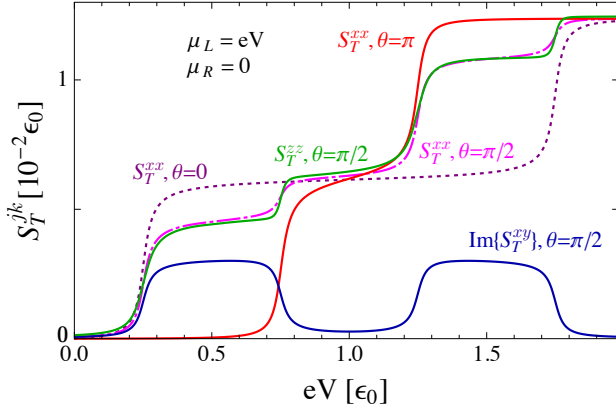


FIG. 6. (Color online) Spin-torque shot-noise components S_T^{jk} as functions of the bias voltage eV for $\mu_R = 0$, $\mu_L = eV$. All plots are obtained at zero temperature, with $\vec{B} = B\vec{e}_z$, and $\Gamma_L = \Gamma_R = \Gamma/2$, for $\Gamma = 0.05\epsilon_0$. The other parameters are set to $\omega_L = 0.5\epsilon_0$, $J = 0.01\epsilon_0$, and $S = 100$. The molecular quasienergy levels lie at $\epsilon_1 = 0.25\epsilon_0$, $\epsilon_2 = 0.75\epsilon_0$, $\epsilon_3 = 1.25\epsilon_0$, and $\epsilon_4 = 1.75\epsilon_0$.

channels and inelastic spin-flip processes. The magnitude of the torque noise at resonance energies ϵ_i , $i = 1, 2, 3, 4$, is determined by θ . In cases $\theta = 0$ and $\theta = \pi$, there are only two transport channels of opposite spins determined by the resulting Zeeman field $B \pm JS/g\mu_B$. The component S_T^{xx} shows two steps with equal heights located at these resonances, where the only contribution to the spin-torque noise comes from elastic tunneling events (dotted purple and red lines in Fig. 6). For $\theta = \pi/2$, the elastic tunneling contributes with four steps with equal heights located at resonances ϵ_i , but due to the contributions of the inelastic precession-assisted processes between quasienergy levels $\epsilon_1(\epsilon_3)$ and $\epsilon_2(\epsilon_4)$, the heights of the steps in S_T^{xx} are not equal anymore (dot-dashed pink line in Fig. 6). Here, we observed that the contribution of the inelastic tunneling processes to S_T^{xx} , involving absorption of an energy quantum ω_L and a spin-flip, shows steps at spin-down quasienergy levels ϵ_1 and ϵ_3 , while it is constant between and after the bias has passed these levels. The component S_T^{zz} shows similar behavior (green line in Fig. 6). As in the case of the inelastic tunneling involving the absorption of one energy quantum ω_L , in $S_T^{xx} = S_T^{yy}$ we observed inelastic spin-flip processes involving the absorption of two energy quanta $2\omega_L$ in the form of steps at spin-down levels ϵ_1 , ϵ_3 , $\epsilon_2 - 2\omega_L$, and $\epsilon_4 - 2\omega_L$, which have negligible contribution compared to the other terms. These processes are a result of correlations of two oscillating spin-currents. For large bias voltage, the spin-torque noise components S_T^{xx} and S_T^{zz} saturate.

The behavior of the component $\text{Im}\{S_T^{xy}\}$ is completely different in nature. It is contributed only by one energy quantum ω_L absorption (emission) spin-flip processes. Interestingly, we obtained the following relation between the Gilbert damping parameter α ,^{42,43} and $\text{Im}\{S_T^{xy}\}$ at

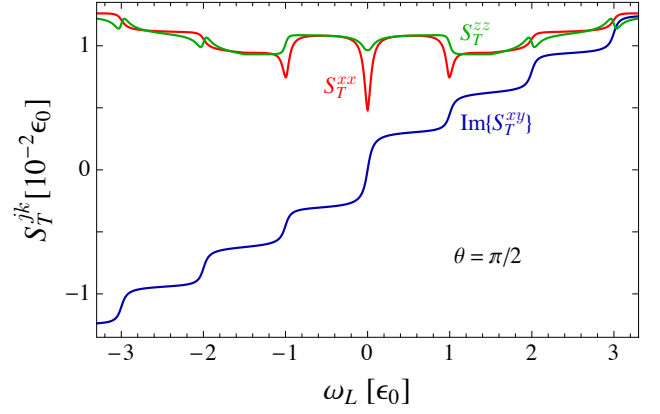


FIG. 7. (Color online) Spin-torque shot-noise components S_T^{jk} as functions of the Larmor frequency ω_L for $\theta = \pi/2$, $\mu_R = 0$, and $\mu_L = 1.5\epsilon_0$. All plots are obtained for $\vec{B} = B\vec{e}_z$ at zero temperature. The other parameters are $\Gamma_L = \Gamma_R = \Gamma/2$, $\Gamma = 0.05\epsilon_0$, $J = 0.01\epsilon_0$, and $S = 100$.

arbitrary temperature

$$\text{Im}\{S_T^{xy}\} = \frac{\omega_L S \sin^2(\theta)}{2} \alpha. \quad (32)$$

Hence, the component $\text{Im}\{S_T^{xy}\}$ is increased for Fermi levels of the leads positioned in the regions where inelastic tunneling processes occur (blue line in Fig. 6).

The spin-torque noise is influenced by the magnetic field \vec{B} since it determines the spin-up and spin-down molecular quasienergy levels. The dependence of S_T^{xx} , $\text{Im}\{S_T^{xy}\}$, and S_T^{zz} on the Larmor frequency ω_L is depicted in Fig. 7. The steps, dips, or peaks in the plots are located at resonant tunneling frequencies $\omega_L = \pm|2\mu_{L,R} - 2\epsilon_0 \pm JS|$. For $\omega_L = 0$ there are only two transport channels, one at energy $\epsilon_0 + JS/2$, which is equal to the Fermi energy of the left lead, and the other at $\epsilon_0 - JS/2$ located between μ_L and μ_R . The contributions of the elastic spin transport processes through these levels result in dips in the components S_T^{xx} and S_T^{zz} , while $\text{Im}\{S_T^{xy}\} = 0$. For $\omega = \epsilon_0$ corresponding to $\mu_R = \epsilon_1$ and $\mu_R = \epsilon_4 - 2\omega_L$, both the elastic and spin-flip tunneling events involving the absorption of energy of one quantum ω_L contribute with a dip, while the spin-flip processes involving the absorption of an energy equal to $2\omega_L$ contribute with a peak to the component S_T^{xx} . For $\omega_L = 2\epsilon_0$ and $\omega_L = 3\epsilon_0$ corresponding to $\mu_L = \epsilon_2$ and $\mu_R = \epsilon_3$, both elastic and spin-flip processes with the absorption of an energy equal to ω_L contribute with a step, while the inelastic processes involving the absorption of an energy $2\omega_L$ give negligible contribution to S_T^{xx} . The component S_T^{zz} shows dips at these two points, since here the dominant contribution comes from inelastic tunneling spin-flip events. The component S_T^{zz} is an even function of ω_L , while $\text{Im}\{S_T^{xy}\}$ is an odd function of ω_L . The spin-torque noise S_T^{xx} is an even function of ω_L for $\theta = \pi/2$.

The spin-torque noise components as functions of θ for $\mu_L = \epsilon_3$ and $\mu_R = 0$ at zero temperature are shown in

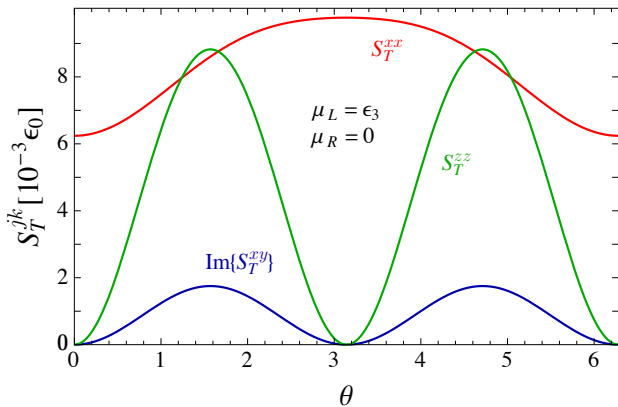


FIG. 8. (Color online) Spin-torque shot-noise components as functions of the tilt angle θ for $\mu_L = \epsilon_3$, $\mu_R = 0$. All plots are obtained at zero temperature, with $\vec{B} = B\vec{e}_z$, $\Gamma = 0.05\epsilon_0$, and $\Gamma_L = \Gamma_R = \Gamma/2$. The other parameters are $\omega_L = 0.5\epsilon_0$, $J = 0.01\epsilon_0$, and $S = 100$.

Fig. 8. The magnitudes and the appearance of the spin-torque noise components at resonance energies ϵ_i can be controlled by θ , since it influences the polarization of the spin current. Here we see that both S_T^{zz} and $\text{Im}\{S_T^{xy}\}$ are zero for $\theta = 0$ and $\theta = \pi$, as the molecular spin is static and its magnitude is constant along z direction in both cases. These torque-noise components take their maximum values for $\theta = \pi/2$, where both elastic and inelastic tunneling contributions are maximal. The component S_T^{xx} takes its minimum value for $\theta = 0$ and its maximum value for $\theta = \pi$, with only elastic tunneling contributions in both cases. For $\theta = \pi/2$, the inelastic tunneling events make a maximal contribution while energy conserving processes give minimal contribution to S_T^{xx} .

V. CONCLUSIONS

In this article, we studied theoretically the noise of charge and spin transport through a small junction, con-

sisting of a single molecular orbital in the presence of a molecular spin precessing with Larmor frequency ω_L in a constant magnetic field. The orbital is connected to two Fermi leads. We used the Keldysh nonequilibrium Green's functions method to derive the noise components of charge and spin currents and spin-transfer torque.

Then, we analyzed the shot noise of charge current and observed characteristics that differ from the ones in the current. In the noise power, we observed diplike features which we attribute to inelastic processes, due to the molecular spin precession, leading to the quantum-interference effect between correlated transport channels.

Since the inelastic tunneling processes lead to a spin-transfer torque acting on the molecular spin, we have also investigated the spin-torque noise components contributed by these processes, involving the change of energy by an energy quantum ω_L . The spin-torque noise components are driven by both the bias voltage and the molecular spin precession. The in-plane noise components S_T^{xx} and S_T^{yy} are also contributed by the processes involving the absorption of an energy equal to $2\omega_L$. We obtained the relation between $\text{Im}\{S_T^{xy}\}$ and the Gilbert damping coefficient α at arbitrary temperature.

Taking into account that the noise of charge and spin transport can be controlled by the parameters such as bias voltage and external magnetic field, our results might be useful in molecular electronics and spintronics. The experimental observation of the predicted noise properties might be a challenging task due to complicated tunnelling processes through molecular magnets. Finding a way to control the spin states of single-molecule magnets in tunnel junctions could be one of the future tasks.

ACKNOWLEDGMENTS

We would like to thank Fei Xu for useful discussions. We gratefully acknowledge the financial support from the Deutsche Forschungsgemeinschaft through the SFB 767 *Controlled Nanosystems*, the Center of Applied Photonics, the DAAD through a STIBET scholarship, and an ERC Advanced Grant *UltraPhase* of Alfred Leitenstorfer.

APPENDIX: FORMAL EXPRESSION FOR THE NONSYMMETRIZED NOISE

Here, we present the derivation of the formal expression for the nonsymmetrized noise $S_{\xi\xi}^{\nu\mu}(t, t')$. The correlation functions $S_{\xi\xi}^{\sigma\sigma', \lambda\eta}(t, t')$, introduced in Eq. (11), can be expressed by means of the Wick's theorem⁵⁶ as

$$\begin{aligned} S_{\xi\xi}^{\sigma\sigma', \lambda\eta}(t, t') &= \sum_{kk'} [V_{k\xi} V_{k'\zeta} G_{\sigma', k'\lambda\zeta}^>(t, t') G_{\eta, k\sigma\xi}^<(t', t) \\ &\quad - V_{k\xi} V_{k'\zeta}^* G_{\sigma', \lambda}^>(t, t') G_{k'\eta\zeta, k\sigma\xi}^<(t', t) \\ &\quad - V_{k\xi}^* V_{k'\zeta} G_{k\sigma'\xi, k'\lambda\zeta}^>(t, t') G_{\eta\sigma}^<(t', t) \\ &\quad + V_{k\xi}^* V_{k'\zeta} G_{k\sigma'\xi, \lambda}^>(t, t') G_{k'\eta\zeta, \sigma}^<(t', t)], \end{aligned} \quad (\text{A1})$$

with the mixed Green's functions defined, using units in which $\hbar = e = 1$, as

$$G_{\eta, k\sigma\xi}^<(t, t') = i \langle \hat{c}_{k\sigma\xi}^\dagger(t') \hat{d}_\eta(t) \rangle, \quad (\text{A2})$$

$$G_{\sigma', k'\lambda\zeta}^>(t, t') = -i \langle \hat{d}_{\sigma'}(t) \hat{c}_{k'\lambda\zeta}^\dagger(t') \rangle, \quad (\text{A3})$$

while Green's functions $G_{k\sigma\xi, \eta}^<(t, t') = -[G_{\eta, k\sigma\xi}^<(t', t)]^*$ and $G_{k'\lambda\zeta, \sigma'}^>(t, t') = -[G_{\sigma', k'\lambda\zeta}^>(t', t)]^*$. The Green's functions of the leads and the central region are defined as

$$G_{k\sigma\xi, k'\sigma'\zeta}^<(t, t') = i \langle \hat{c}_{k'\sigma'\zeta}^\dagger(t') \hat{c}_{k\sigma\xi}(t) \rangle, \quad (\text{A4})$$

$$G_{k\sigma\xi, k'\sigma'\zeta}^>(t, t') = -i \langle \hat{c}_{k\sigma\xi}(t) \hat{c}_{k'\sigma'\zeta}^\dagger(t') \rangle, \quad (\text{A5})$$

$$G_{\sigma\sigma'}^<(t, t') = i \langle \hat{d}_{\sigma'}^\dagger(t') \hat{d}_\sigma(t) \rangle, \quad (\text{A6})$$

$$G_{\sigma\sigma'}^>(t, t') = -i \langle \hat{d}_\sigma(t) \hat{d}_{\sigma'}^\dagger(t') \rangle, \quad (\text{A7})$$

$$G_{\sigma\sigma'}^{r,a}(t, t') = \mp i \theta(\pm t \mp t') \langle \hat{d}_\sigma(t), \hat{d}_{\sigma'}^\dagger(t') \rangle. \quad (\text{A8})$$

Since the self-energies originating from the coupling between the electronic level and the lead ξ are diagonal in the electron spin space, their entries can be written as $\Sigma_\xi^{<,>,r,a}(t, t') = \sum_k V_{k\xi} g_{k\xi}^{<,>,r,a}(t, t') V_{k\xi}^*$, where $g^{<,>,r,a}(t, t')$ are the Green's functions of the free electrons in lead ξ . Applying Langreth analytical continuation rules,⁵⁷ Eq. (A1) transforms into

$$\begin{aligned} S_{\xi\xi}^{\sigma\sigma', \lambda\eta}(t, t') &= \int dt_1 \int dt_2 \\ &\quad \times \{ [G_{\sigma', \lambda}^r(t, t_1) \Sigma_\zeta^>(t_1, t') + G_{\sigma', \lambda}^>(t, t_1) \Sigma_\zeta^a(t_1, t')] [G_{\eta\sigma}^r(t', t_2) \Sigma_\xi^<(t_2, t) + G_{\eta\sigma}^<(t', t_2) \Sigma_\xi^a(t_2, t)] \\ &\quad + [\Sigma_\xi^>(t, t_1) G_{\sigma', \lambda}^a(t_1, t') + \Sigma_\xi^r(t, t_1) G_{\sigma', \lambda}^>(t_1, t')] [\Sigma_\zeta^<(t', t_2) G_{\eta\sigma}^a(t_2, t) + \Sigma_\zeta^r(t', t_2) G_{\eta\sigma}^<(t_2, t)] \\ &\quad - G_{\sigma', \lambda}^>(t, t') [\Sigma_\zeta^r(t', t_1) G_{\eta\sigma}^r(t_1, t_2) \Sigma_\xi^<(t_2, t) + \Sigma_\zeta^<(t', t_1) G_{\eta\sigma}^a(t_1, t_2) \Sigma_\xi^a(t_2, t) \\ &\quad + \Sigma_\zeta^r(t', t_1) G_{\eta\sigma}^<(t_1, t_2) \Sigma_\xi^a(t_2, t)] - [\Sigma_\xi^r(t, t_1) G_{\sigma', \lambda}^r(t_1, t_2) \Sigma_\zeta^>(t_2, t') \\ &\quad + \Sigma_\xi^>(t, t_1) G_{\sigma', \lambda}^a(t_1, t_2) \Sigma_\zeta^a(t_2, t') + \Sigma_\xi^r(t, t_1) G_{\sigma', \lambda}^>(t_1, t_2) \Sigma_\zeta^a(t_2, t')] G_{\eta\sigma}^<(t', t) \} \\ &\quad - \delta_{\xi\xi} [\delta_{\eta\sigma} G_{\sigma', \lambda}^>(t, t') \Sigma_\xi^<(t', t) + \delta_{\sigma', \lambda} \Sigma_\xi^>(t, t') G_{\eta\sigma}^<(t', t)]. \end{aligned} \quad (\text{A9})$$

Finally, using Eqs. (11) and (A9), the obtained formal expression for the nonsymmetrized noise of charge current^{40,58} and spin currents in standard coordinates t and t' can be written as

$$\begin{aligned} S_{\xi\xi}^{\nu\mu}(t, t') &= -\frac{q_\nu q_\mu}{\hbar^2} \text{Tr} \left\{ \int dt_1 \int dt_2 \right. \\ &\quad \times \{ \hat{\sigma}_\nu [\hat{G}^r(t, t_1) \hat{\Sigma}_\zeta^>(t_1, t') + \hat{G}^>(t, t_1) \hat{\Sigma}_\zeta^a(t_1, t')] \hat{\sigma}_\mu [\hat{G}^r(t', t_2) \hat{\Sigma}_\xi^<(t_2, t) + \hat{G}^<(t', t_2) \hat{\Sigma}_\xi^a(t_2, t)] \\ &\quad + \hat{\sigma}_\nu [\hat{\Sigma}_\xi^>(t, t_1) \hat{G}^a(t_1, t') + \hat{\Sigma}_\xi^r(t, t_1) \hat{G}^>(t_1, t')] \hat{\sigma}_\mu [\hat{\Sigma}_\zeta^<(t', t_2) \hat{G}^a(t_2, t) + \hat{\Sigma}_\zeta^r(t', t_2) \hat{G}^<(t_2, t)] \\ &\quad - \hat{\sigma}_\nu \hat{G}^>(t, t') \hat{\sigma}_\mu [\hat{\Sigma}_\zeta^r(t', t_1) \hat{G}^r(t_1, t_2) \hat{\Sigma}_\xi^<(t_2, t) + \hat{\Sigma}_\zeta^<(t', t_1) \hat{G}^a(t_1, t_2) \hat{\Sigma}_\xi^a(t_2, t) + \hat{\Sigma}_\zeta^r(t', t_1) \hat{G}^<(t_1, t_2) \hat{\Sigma}_\xi^a(t_2, t)] \\ &\quad - \hat{\sigma}_\nu [\hat{\Sigma}_\xi^r(t, t_1) \hat{G}^r(t_1, t_2) \hat{\Sigma}_\zeta^>(t_2, t') + \hat{\Sigma}_\xi^>(t, t_1) \hat{G}^a(t_1, t_2) \hat{\Sigma}_\zeta^a(t_2, t') + \hat{\Sigma}_\xi^r(t, t_1) \hat{G}^>(t_1, t_2) \hat{\Sigma}_\zeta^a(t_2, t')] \hat{\sigma}_\mu \hat{G}^<(t', t) \} \\ &\quad \left. - \delta_{\xi\xi} \hat{\sigma}_\nu [\hat{G}^>(t, t') \hat{\sigma}_\mu \hat{\Sigma}_\xi^<(t', t) + \hat{\Sigma}_\xi^>(t, t') \hat{\sigma}_\mu \hat{G}^<(t', t)] \right\}, \end{aligned} \quad (\text{A10})$$

where Tr denotes the trace in the electronic spin space.

-
- ¹ Y. M. Blanter and M. Büttiker, *Physics Reports*, **336**, 2 (2000).
- ² E. G. Mishchenko, *Phys. Rev. B* **68**, 100409(R) (2003).
- ³ W. Belzig and M. Zareyan, *Phys. Rev. B* **69**, 140407 (2004).
- ⁴ F. M. Souza, A. P. Jauho, and J. C. Egues, *Phys. Rev. B* **78**, 155303 (2008).
- ⁵ A. E. Miroschnichenko, S. Flach, and Y. S. Kivshar, *Rev. Mod. Phys.* **82**, 2257 (2010).
- ⁶ C. M. Guédon, H. Valkenier, T. Markussen, K. S. Thygesen, J. C. Hummelen, and S. J. van der Molen, *Nature Nanotech.* **7**, 305 (2012).
- ⁷ H. Vázquez, R. Skouta, S. Schneebeli, M. Kamenetska, R. Beslov, L. Venkataraman, and M. S. Hybertsen, *Nature Nanotech.* **7**, 663 (2012).
- ⁸ R. Stadler, *Phys. Rev. B* **80**, 125401 (2009).
- ⁹ M. A. Ratner, *J. Phys. Chem.* **94**, 4877 (1990).
- ¹⁰ T. Hansen, G. C. Solomon, D. Q. Andrews, and M. A. Ratner, *J. Chem. Phys.* **131**, 194704 (2009).
- ¹¹ U. Fano, *Phys. Rev.* **124**, 1866 (1961).
- ¹² J. Faist, F. Capasso, C. Sirtori, K. W. West, and L. N. Pfeiffer, *Nature* **390**, 589 (1997).
- ¹³ O. Entin-Wohlman, Y. Imry, S. A. Gurvitz, and A. Aharony, *Phys. Rev. B* **75**, 193308 (2007).
- ¹⁴ D. Sánchez and L. Serra, *Phys. Rev. B* **74**, 153313 (2006).
- ¹⁵ Piotr Stefański, *J. Phys.: Cond. Matter* **22**, 505303 (2010).
- ¹⁶ B. H. Wu and C. Timm, *Phys. Rev. B* **81**, 075309 (2010).
- ¹⁷ S. A. Gurvitz, D. Mozyrsky, and G. P. Berman, *Phys. Rev. B* **72**, 205341 (2005).
- ¹⁸ S. A. Gurvitz, *IEEE Trans. Nanotechnology* **4**, 45 (2005).
- ¹⁹ D. Mozyrsky, L. Fedichkin, S. A. Gurvitz, and G. P. Berman, *Phys. Rev. B* **66**, 161313 (2002).
- ²⁰ A. Lamacraft, *Phys. Rev. B* **69**, 081301(R) (2004).
- ²¹ M. Zareyan and W. Belzig, *Europhys. Lett.* **70**, 817 (2005).
- ²² B. Wang, J. Wang, and H. Guo, *Phys. Rev. B* **69**, 153301 (2004).
- ²³ S. H. Ouyang, C. H. Lam, and J. Q. You, *Euro. Phys. J. B* **64**, 67 (2008).
- ²⁴ O. Sauret and D. Feinberg, *Phys. Rev. Lett.* **92**, 106601 (2004).
- ²⁵ M. J. Stevens, A. L. Smirl, R. D. R. Bhat, A. Najmale, J. E. Sipe, and H. M. van Driel, *Phys. Rev. Lett.* **90**, 136603 (2003).
- ²⁶ A. Brataas, Y. Tserkovnyak, G. E. W. Bauer, and B. I. Halperin, *Phys. Rev. B* **66**, 060404(R) (2002).
- ²⁷ R. L. Dragomirova and B. K. Nikolić, *Phys. Rev. B* **75**, 085328 (2007).
- ²⁸ Y. He, D. Hou, and R. Han, *J. Appl. Phys.* **101**, 023710 (2007).
- ²⁹ Y. Yu, H. Zhan, L. Wan, B. Wang, Y. Wei, Q. Sun and J. Wang, *Nanotechnology* **24**, 155202 (2013).
- ³⁰ J. Foros, A. Brataas, Y. Tserkovnyak, and G. E. W. Bauer, *Phys. Rev. Lett.* **95**, 016601 (2005).
- ³¹ A. L. Chudnovskiy, J. Swiebodzinski, and A. Kamenev, *Phys. Rev. Lett.* **101**, 066601 (2008).
- ³² A. Kamra, F. P. Witek, S. Meyer, H. Huebl, S. Geprägs, R. Gross, G. E. W. Bauer, and S. T. B. Goennenwein, *Phys. Rev. B* **90**, 214419 (2014).
- ³³ A. Kamra and W. Belzig, *Phys. Rev. Lett.* **116**, 146601 (2016); *Phys. Rev. B* **94**, 014419 (2016).
- ³⁴ A. Kamra and W. Belzig, *Phys. Rev. Lett.* **119**, 197201 (2017).
- ³⁵ Y. Wang and L. J. Sham, *Phys. Rev. B* **85**, 092403 (2012).
- ³⁶ Y. Wang and L. J. Sham, *Phys. Rev. B* **87**, 174433 (2013).
- ³⁷ J. C. Slonczewski, *J. Magn. Magn. Mater.* **159**, L1 (1996).
- ³⁸ L. Berger, *Phys. Rev. B* **54**, 9353 (1996).
- ³⁹ A.-P. Jauho, N. S. Wingreen, and Y. Meir, *Phys. Rev. B* **50**, 5528 (1994).
- ⁴⁰ A.-P. Jauho and H. Haug, *Quantum Kinetics in Transport and Optics of Semiconductors* (Springer, Berlin, 2008).
- ⁴¹ N. S. Wingreen, A.-P. Jauho, and Y. Meir, *Phys. Rev. B* **48**, 8487 (1993).
- ⁴² M. Filipović, C. Holmqvist, F. Haupt, and W. Belzig, *Phys. Rev. B* **87**, 045426 (2013); **88**, 119901(E) (2013).
- ⁴³ M. Filipović and W. Belzig, *Phys. Rev. B* **93**, 075402 (2016).
- ⁴⁴ T. L. Gilbert, *Phys. Rev.* **100**, 1243 (1955); T. Gilbert, *IEEE Trans. Magn.* **40**, 3443 (2004).
- ⁴⁵ Y. Tserkovnyak, A. Brataas, G. E. W. Bauer, and B. I. Halperin, *Rev. Mod. Phys.* **77**, 1375 (2005).
- ⁴⁶ D. C. Ralph and M. D. Stiles, *J. Magn. and Magn. Mater.* **320**, 1190 (2008).
- ⁴⁷ C. Kittel, *Phys. Rev.* **73**, 155 (1948).
- ⁴⁸ M. H. Pedersen and M. Büttiker, *Phys. Rev. B* **58**, 12993 (1998).
- ⁴⁹ B. Wang, J. Wang, and H. Guo, *Phys. Rev. B* **67**, 092408 (2003).
- ⁵⁰ N. Bode, L. Arrachea, G. S. Lozano, T. S. Nunner, and F. von Oppen, *Phys. Rev. B* **85**, 115440 (2012).
- ⁵¹ G. Floquet, *Ann. Sci. Ecole Normale Supérieure* **12**, 47 (1883).
- ⁵² Jon H. Shirley, PhD Thesis, California Institute of Technology, (1963).
- ⁵³ M. Grifoni and P. Hänggi, *Phys. Rep.* **304**, 229 (1998).
- ⁵⁴ S.-I. Chu and D. A. Telnov, *Phys. Rep.* **390**, 1 (2004).
- ⁵⁵ A. Thielmann, M. H. Hettler, J. König, and G. Schön, *Phys. Rev. B* **68**, 115105 (2003).
- ⁵⁶ A. Fetter and J. D. Walecka, *Quantum Theory of Many-Particle Systems* (Dover Publications, Inc., Mineola, N. Y., 2003).
- ⁵⁷ D. C. Langreth, in *Linear and Nonlinear Electron Transport in Solids*, edited by J. T. Devreese and E. Van Doren (Plenum, New York, 1976).
- ⁵⁸ Z. Feng, J. Maciejko, J. Wang, and H. Guo, *Phys. Rev. B* **77**, 075302 (2008).